

Assessment of Adsorption Properties of Neem Leaves Wastes for the Removal of Congo Red and Methyl Orange

Muhammad B. Ibrahim¹ Muhammad S. Sulaiman¹ and Sadiq Sani²

Abstract—Neem leaves were studied as plant wastes derived adsorbents for detoxification of Congo Red (CR) and Methyl Orange (MO) from aqueous solutions using batch adsorption technique. The objectives involved determining the effects of the basic adsorption parameters namely, agitation time, adsorbent dosage, adsorbents particle size, adsorbate loading concentrations and initial pH, on the adsorption process as well as characterizing the adsorbents by determining their physicochemical properties, functional groups responsible for the adsorption process using Fourier Transform Infrared (FTIR) spectroscopy and surface morphology using scanning electron microscopy (SEM) coupled with energy dispersive X-ray spectroscopy (EDS). The adsorption behaviours of the materials were tested against Langmuir, Freundlich, Temkin, Dubinin Radushkevich and Harkins Jura isotherm models. Percent adsorption increased with increase in agitation time (5 – 240 minutes), adsorbent dosage (100-500mg), initial concentration (100-300mg/L), and with decrease in particle size ($\geq 75\mu\text{m}$ to $\leq 300\mu\text{m}$) of the adsorbents. Both processes are dye pH-dependent, increasing or decreasing percent adsorption in acidic (2-6) or alkaline (8-12) range over the studied pH (2-12) range. From the experimental data the Langmuir's separation factor (R_L) suggests unfavourable adsorption for all processes, Freundlich constant (n_F) indicates unfavourable process for CR and MO adsorption; while the mean free energy of adsorption E , calculated from Dubinin-Radushkevich equation suggest a physical adsorption. Reduction in band intensities and vibrational changes observed in FTIR spectra indicate possible involvement of carbonyl (-C=O), carboxyl (-COOH) and hydroxyl (-OH) functional groups on the adsorbents' surfaces during the adsorption and interaction with the sulfonic acid groups ($\text{-SO}_3\text{Na}$) on the dye molecules. The difference in irregular and porous texture surface morphology of fresh and dye-loaded adsorbent characterized the adsorption of the dyes by the adsorbent. While EDS analysis indicates that adsorbent consist of mainly C and O, and small amounts of, Ca, Mg, K, P and S. The result of this study shows that neem leaves are potential alternative low-cost adsorbents for the effective removal of Congo red (CR) and methyl orange (MO), from aqueous solutions.

Keywords—Adsorption, Congo red, Methyl orange, Neem Leaves

Muhammad B. Ibrahim and Muhammad S. Sulaiman¹ are with the Department of Pure and Industrial Chemistry, Bayero University, P.M.B. 3011, Kano, Nigeria.

Sadiq Sani², is with Department of Applied Chemistry, Federal University Dutsin-Ma, P.M.B. 5001, Katsina, Nigeria.

I. INTRODUCTION

THE search for new technologies involving the removal of toxic substances from wastewaters has directed attention to biosorption based on binding capacities of various biological materials [1]. Though the use of biomass for environmental purposes has been in practice for long, researchers are hopeful that the method will lead to an alternative economical method for the removal of heavy toxic substances from wastewater. The efficiency of biomass depends on factors such as number of sites on the biosorbent material, their accessibility and chemical state, and the affinity between sites and metals [2]. Water pollution by dyes is believed to begin during the earliest use of colorants by the Neanderthal man about 180,000 years ago [3]. However, modern water pollution by dye could be traced back to the years that followed historic discovery of first synthetic dye.

Various low-cost adsorbents that have been successfully employed for the adsorption of dyes from wastewater include chitosan [4], modified agricultural byproducts [5], natural and modified clay minerals [6], maize cob, peat, sawdust, coal, baggase, neem leaves, [7] – [9] watermelon rind [6], [10]. Vimonses *et al.* [11] investigated the adsorption of Congo red on zeolite, kaolin and bentonite. Results revealed that zeolite among the three clay minerals showed least adsorption of Congo red. Wong *et al.* [12] analysed the adsorption of acidic dyes on chitosan. The amount of Acid Orange 12, Acid Orange 10, Acid Red 73, Acid Red 18 and Acid Green 25 adsorbed on chitosan was reported as 973.3, 922.9, 728.2, 693.2 and 645.1mgg^{-1} respectively. *Azadirachta indica* (Neem) leaf powder was used as a biosorbent for removal of Cadmium (II) from aqueous medium by Sharma and Bhattacharyya [13]. Adsorption increased from 8.8% at pH 4.0 to 70.0% at pH 7.0 and 93.6% at pH 9.5, the higher values in alkaline medium being due to removal by precipitation. The adsorption was very fast initially and maximum adsorption was observed within 300 min of agitation.

II. MATERIALS AND METHODS

A. Preparation of Adsorbent Samples

Preparation of adsorbent samples was done according to Sharma *et al.* [14] and Gopalakrishnan *et al.* [15]: Neem leaves samples collected were thoroughly washed with tap-water, rinsed copiously with distilled water to remove dust and any other soluble substances. The leaves were allowed to dry

for seven days in the laboratory at room temperature until they became crisp. The dried leaves samples were then pulverized with a mechanical electronic grinder into fine powder and then dried for 16 hours in an oven at 65°C. The oven-dried neem leaves powder (NLP) samples were sieved to the working sizes of ≤75 μm, ≤150 μm, ≤250 μm, ≤300 μm and >300 μm using electronic shaker.

B. Physicochemical Properties of Adsorbent Material

Determination of moisture, ash and organic matter contents of the adsorbent were carried in accordance to procedures obtained from the literature Sluiter *et al.* [16]: Moisture content was determined by introducing 15g sample of the adsorbent into a clean crucible of weight w₁, and the initial weight of the adsorbent and crucible was recorded as w₂. The adsorbent was introduced into oven and dried to constant mass at 115°C for 16 hours; and the final weight was recorded as w₃. The determination was carried out in triplicates, reporting moisture content as the mean of the recorded percentage weight of the evaporated sample on oven-dry weight basis using the relationship in Equation 1.

$$\% \text{ Moisture Content} = \frac{w_2 - w_3}{w_2 - w_1} \times 100 \dots \dots \dots 1$$

where (w₂ – w₃) is the weight of evaporated water, (w₂ – w₁) the oven-dry weight of the sample, w₁ is the weight of empty dried crucible, w₂ the weight of sample and crucible before heating and w₃ the weight of sample and crucible after heating.

Ash content of the adsorbent sample was determined by placing a marked 50cm³ ashing porcelain crucible in a muffle furnace at 600°C for a period of four hours. After ashing, the crucible was cooled for one hour, then directly transferred from the furnace into desiccator. The weight of the crucible was then measured and recorded to the nearest 0.1 mg as w_a. A 10g NLP sample, oven-dried at 105°C and stored in desiccators, was weighed into the ashed crucible and initial weight of crucible with sample recorded as w_b, and then introduced into the muffle furnace and ashed at 600°C for 4 hours to a constant weight (change of less than ± 0.3 mg) and final weight of crucible with sample recorded as w_c. The percentage ash content was calculated using Equation 2.

$$\% \text{ Ash Content} = \frac{w_b - w_c}{w_b - w_a} \times 100 \dots \dots \dots 2$$

where (w_b – w_c) is the weight of the ashed sample without the crucible and (w_b – w_a) the weight of the oven-dry sample without the crucible.

The organic matter contents of the adsorbents were determined from the difference between 100% oven-dried adsorbent and the percentage ash contents as illustrated in Equation 3.

$$\% \text{ Organic Matter content} = 100 - \% \text{ Ash content} \dots \dots \dots 3$$

C. Batch Adsorption and Optimisation Studies

Experiments on the adsorption of CR and MO by NLP were carried out by batch method for which the influence of various parameters such as agitation time (5 – 240 min), adsorbent dosage (100 – 500mg), particle size, initial dye concentration (5 – 300mg/L) and initial dye pH (2 - 12) were studied at constant agitation speed of 300 rpm and room temperature

(25°C) in triplicates. The adsorption measurements were conducted by mixing specified amount of adsorbent in 150cm³ Erlenmeyer flasks containing 50 cm³ of dye solution of known concentration. The initial pH of the dye solutions were adjusted to the desired values by adding few drops of 0.1M HCl or 0.1M NaOH aqueous solutions. The solutions were agitated using an orbital shaker for a predetermined time to attain equilibrium; after which the samples were taken out and the supernatant solution was separated from the adsorbent by filtration with Whatman No. 41 filter paper, discarding the first few volume (3-4 drops) of the filtrate. The filtrates were analysed using UV-vis spectrophotometer at λ_{max} of 496.5nm for CR and 464nm for MO, for residual dye concentration; reporting each data as an average value of the triplicate readings. The percentage adsorption and substrate’s equilibrium adsorption capacity, q_e (mg/g) were evaluated using Equations 4 and 5 respectively.

$$\% \text{ Adsorption} = \frac{C_o - C_e}{C_o} \times 100 \dots \dots \dots 4$$

$$q_e = \frac{C_o - C_e}{w} \times V \dots \dots \dots 5$$

where C_o (mg/L) is the initial dye concentration, C_e is the concentration at equilibrium or predetermined time t, V (L) is the volume of dye solution used and w (g) is the weight of the adsorbent.

D. Fourier Transform Infra Red (FTIR) Spectroscopy

As characterization of adsorbent’s surface and structure hold keys to understanding the dye binding mechanism onto biomass, FTIR spectroscopy was conducted on both the fresh and dye loaded adsorbents using a CARY 630 FTIR spectrophotometer (Agilent Technologies).

E. Scanning Electron Microscopy (SEM)

NLP samples were examined under scanning electron microscope (SEM) to analyze their morphological and surface characteristics. The SEM was carried out using a Philips XL30 Scanning Electron Microscope at accelerating voltage of 15kV, beam size 3.0, working distance 10 and magnification of 1000. The samples were coated with carbon under vacuum before analysis to prevent the accumulation of static electric charge on the surface of particles.

III. RESULTS AND DISCUSSION

Percentage moisture, ash and organic matter contents of the adsorbent are reported in the form of mean±standard deviation of three readings. The results (Table 1) show that moisture content (7.09 ± 0.32) < ash content (10.87 ± 0.09) < organic matter content (82.04 ± 0.40) for the powdered adsorbent.

TABLE I
PHYSICOCHEMICAL PROPERTIES

Properties	%
Mixture Contents	7.09 ± 0.32
Ash Contents	10.87 ± 0.09
Organic Matter Contents	82.04 ± 0.04

The FTIR spectra of the adsorbent (Fig. 1a – 1c) before and after adsorption indicated significant changes in the observed

peaks; and the respectively assigned functional groups are as enumerated in Appendix 1. SEM and EDX (Energy-dispersive X-ray spectroscopy) are useful analytical tools for evaluating the characteristics of adsorbent materials. SEM micrographs of the neem leaf powder (Fig. 2a – 2c) showed that the powder was an assemblage of fine particles, which did not have regular, fixed shape and size. The surface appears as a fibrous material with irregular macropores and some expanded cavities which may allow for the diffusion of the dye molecules through the macropores of the adsorbent. EDX results (Fig. 3) indicates that Neem leaf powder consist of mainly C and O, and small amounts of, Ca, Mg, K, P and S.

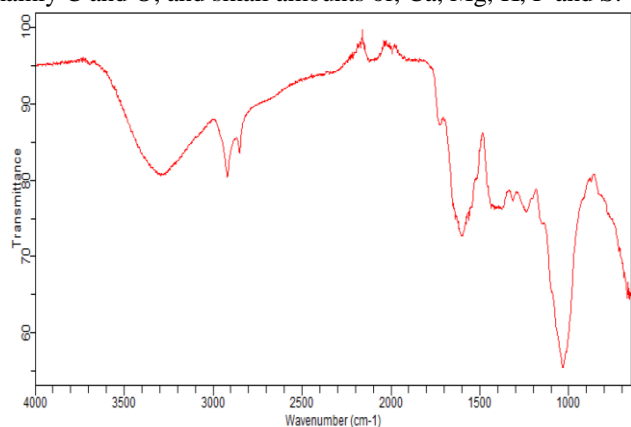


Fig. 1a: Fresh NLP

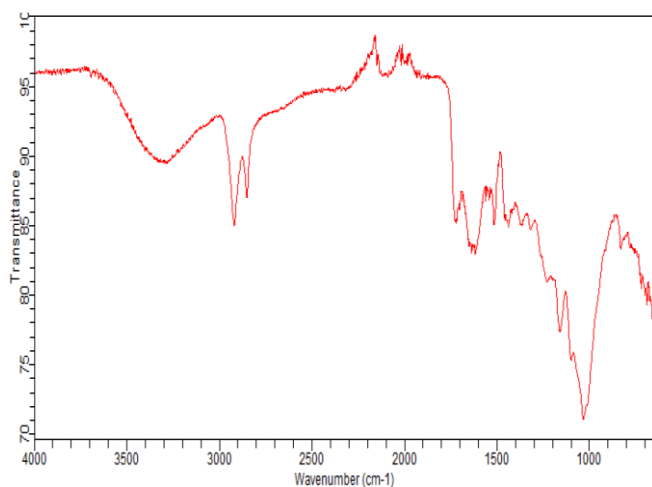


Fig. 1b: Congo Red Loaded NLP

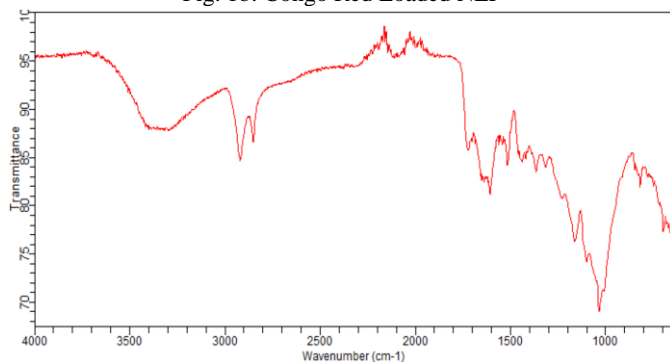


Fig. 1c: Methyl orange Loaded NLP

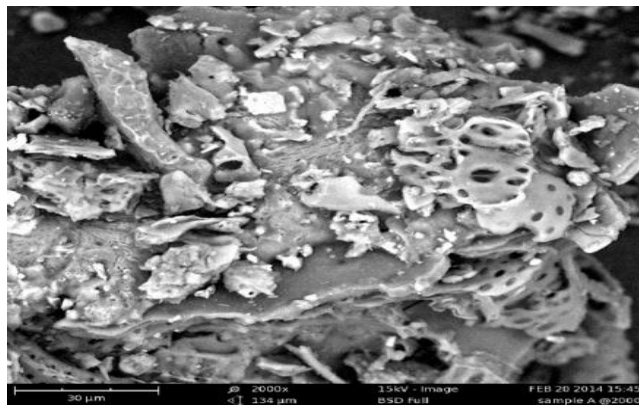


Fig. 2a: NLP Before adsorption

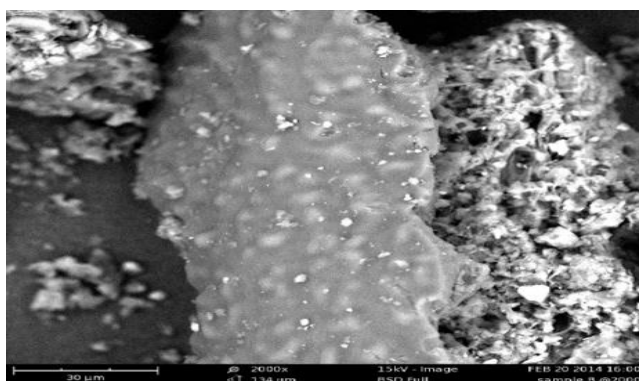


Fig. 2b: CR Loaded NLP

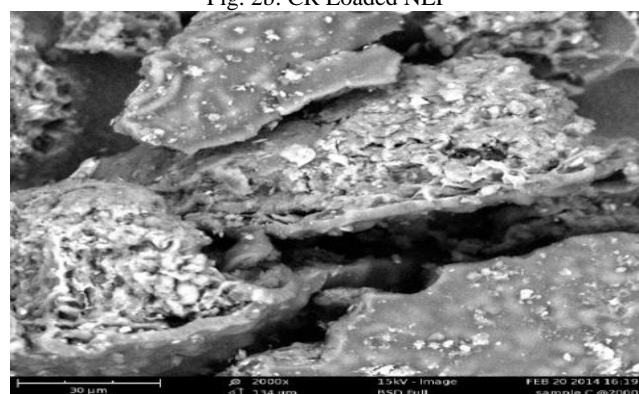


Fig. 2c: MO Loaded NLP

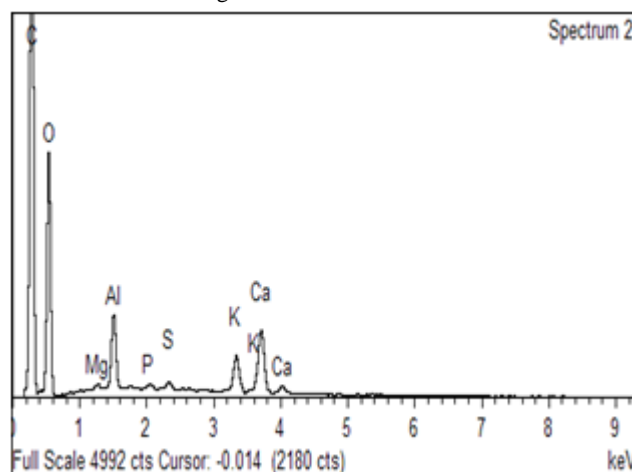


Fig. 3: EDX Image of Neem Leaf Powder

IV. BATCH ADSORPTION AND OPTIMISATION STUDIES

Studies on the effect of agitation time (5 – 240 minutes) on the percent adsorption of the dyes (CR and MO) onto NLP adsorbents were carried out and from the results (Fig. 4) the percent adsorption of the dye was rapid (69.44 - 99.70%) within 5 to 15 minutes until attained an optimum (99.70%) in 15 minutes and equilibrium (96.32%) in 45 minutes. Similarly, the percent adsorption of MO onto NLP was fast (66.85-80.33%) within 5 to 45 minutes attaining an optimum (83.33%) at 45 minutes and equilibrium (64.79%) in 120 minutes.

Agitation time is an important parameter that affects all transfer phenomena including adsorption process. According to Suyamboo and Perumal [17] with increased agitation time, the rate of diffusion of the dye molecules from bulk liquid to the liquid - adsorbent interphase becomes higher due to enhanced turbulence and decreased thickness of the interphase layer. The relatively high removal of dye initially by the adsorbents could be attributed to the availability of large number of vacant sites for adsorption of Congo red and methyl orange onto surfaces of the adsorbents. Lian *et al.* [18] reported similar results for the adsorption of Congo red on Ca-bentonite. Later, the process becomes relatively slower as it approaches equilibrium conditions until equilibrium is achieved. At this time, the amount of the dye desorbing from the adsorbent is in a state of dynamic equilibrium with the amount of the dye being adsorbed onto the adsorbents. The time required to attain this state of equilibrium is termed the equilibrium time, and the amount of dye adsorbed at the equilibrium time reflects the maximum adsorption capacity of the adsorbent under the working conditions [19].

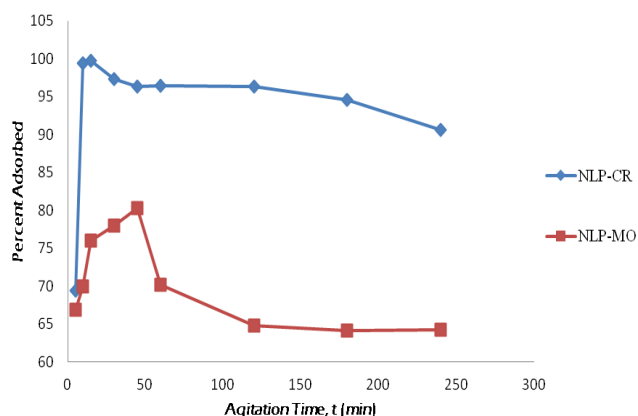


Fig. 4: Variation of % Adsorption with Agitation Time

Effects of adsorbents dosage (100-500mg) on percent adsorption of dyes (CR and MO) has been investigated at predetermined equilibrium agitation times and the results are as presented in Fig. 5, which shows increase with increase in adsorbent dosage from 100-500mg, (NLP: 23.81-57.23%) As amount of adsorbent increases, number of active sites available for adsorption also increases, thus increasing the percent adsorption for dyes. This can be explained by the accessibility of transferrable sites or surface area on adsorbents between the liquid solution phase and the solid phase. At the minimum dosage (0.1g) there was diminutive availability of exchangeable sites which in turn led to removal of minimum

amounts of dyes, while at maximum dosage (0.5g) there was greater availability of exchangeable sites or surface area which ultimately led to the removal of maximum amounts of dyes [15].

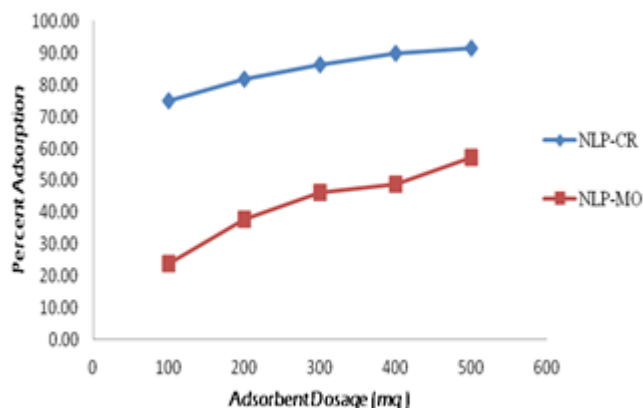


Fig. 5: Variation of % Adsorption with Adsorbent Dosage

Studies on the effect of adsorbates initial concentration (5-300mg/L) on the percent adsorption of the dyes (CR and MO) onto NLP adsorbent were carried out at their respective equilibrium agitation times and the results are as presented in Fig. 6. The percent adsorption of CR onto NLP increased rapidly (21.19-86.69%) within 5mg/L to 100mg/L and then slowly (86.69-90.48%) within 100mg/L to 200mg/L before it decreased (82.43%) at 300mg/L.

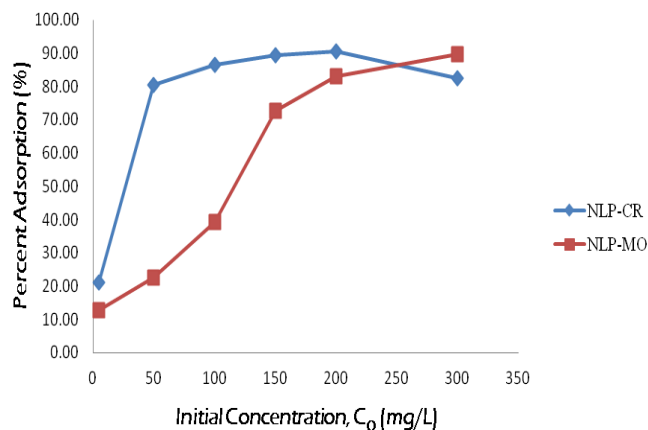


Fig. 6: Variation of % Adsorption with Initial Adsorbate Loading Concentration

Surface areas of biosorbent have a greater influence on metal biosorption, especially when it is higher. Sharma and Bhattacharyya, [13], found the specific surface area of neem leaf powder to be 21.45m²/g. Generally, as the adsorbent particle sizes decrease the surface area increases leading to increased adsorption of dye molecules. Both percent adsorption of Congo red and methyl orange (91.71-83.41%) and (52.83-46.01%) respectively; show good decrease as the adsorbent particle size increases ($\leq 75\mu\text{m}$ to $\geq 300\mu\text{m}$) as depicted in Fig. 7. This can be attributed to the fact that the bigger particle sizes have widened diffusion path and decreased total surface area that lowers the ability of the dye to penetrate the entire internal pore structures of the adsorbents while the smaller particle sizes have shortened diffusion path and increased total surface area that makes the ability of the

dye to penetrate all the internal pore structures of the adsorbents very high.

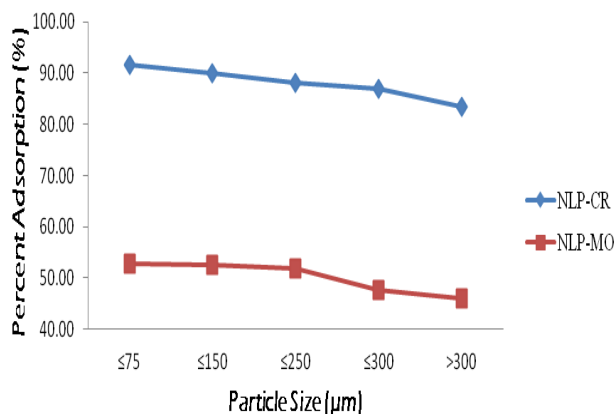


Fig. 7: Variation of % Adsorption with Particle Size

Initial pH of dyes was found to have a profound effect on the percent adsorption of dyes onto the adsorbents. Adsorption of MO by NLP increased fast from 79.87% at pH 2 until it attained the optimum value of 87.92% at pH 4 and decreased fast from 87.92% at pH 4 to 82.42% at pH 7 before it decreased slowly to 81.86 at pH 12.

This rapid increase in percent adsorption of the dyes (CR and MO) by NLP in acidic pH range of 2-6 (88.39-90.97%) and (79.87-87.92%) respectively were similar to that reported for the adsorption of anionic dyes such as methyl orange (MO) onto Lapindo volcanic mud (LVM) [20]. Therefore, performing the adsorption in the acidic medium would increase the positive charge on the adsorbent surface causing an increase in the electrostatic attraction between anionic dye molecules (CR-dye⁻ and MO-dye⁻) and the surface of adsorbents; hence, the increased rate of adsorption of the dyes (CR and MO).

On the other hand, the presence of high concentration of hydroxyl ions (OH⁻) on the adsorbents in the basic medium at pH range of 8-12 compete effectively with anionic dye molecules leading to decreased percent adsorption.

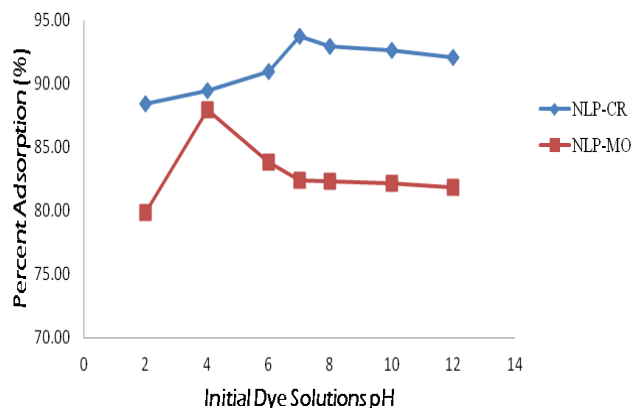


Fig. 8: Effect of Adsorbate pH on % Adsorption

V. ADSORPTION ISOTHERM MODELS

Based on the relationship of adsorption capacity for the dyes adsorption onto the adsorbents and the equilibrium concentrations, the various adsorption isotherms were plotted and the respective parameters of the tested models are as enumerated in Table 2. The values of linear regression coefficient (R^2) are a measure of goodness – of – fit of the adsorption data for each tested isotherm plot.

For Langmuir isotherm the value of the dimensionless parameter R_L is employed to judge the nature of the adsorption process. While for Freundlich isotherm the heterogeneity factor n_F , which represent the deviation from linearity of adsorption is employed. On the other hand, for Temkin, Dubinin – Radushkevich (D – R) and Harkins – Jura isotherms, the energy parameters b_T , E and B_{HJ} expresses the adsorption as physical or chemical.

TABLE II
ADSORPTION ISOTHERM PARAMETERS

Adsorption Isotherm Parameters		Neem-tree Leaves	
		CR	MO
<i>Langmuir</i>	q_m (mg/g)	24.81	21.23
	K_L	-0.4306	-0.1365
	R_L	-0.0078	-0.0250
	R^2	0.9998	0.9989
<i>Freundlich</i>	$ n_F $	3.78	5.47
	K_F	37.3488	50.9732
	R^2	0.9919	0.9910
<i>Temkin</i>	b_T (kJ/mol)	0.7374	-0.5362
	B_T	-2.6164	-4.6209
	A_T	1.11×10^{-6}	9.06×10^{-5}
	R^2	0.9932	0.9937
<i>D - R</i>	B_D (mol ² /J ²)	5×10^{-6}	3×10^{-5}
	E (kJ/mol)	0.3162	0.1291
	q_D (mg/g)	26.06	23.09
	R^2	0.9359	0.9487
<i>Harkins-Jura</i>	A_{HJ}	-1667	-769
	B_{HJ}	-0.8333	0.4615
	R^2	0.9889	0.9837

VI. CONCLUSION

The findings of this work show that Neem leaves biomass which is cheap and abundantly available can be utilised as effective adsorbent, due to its outstanding uptake capacity.

APPENDIX I

FUNCTIONAL GROUP ASSIGNMENT TO OBSERVED FREQUENCIES

S/N	Neem-tree Leaves Wave Numbers of Absorption (cm ⁻¹)			Assignment
	Before Adsorption	CR-loaded	MO-loaded	
1	3295	3289	3419	O-H stretching vibration in carboxylic acid groups (2500-3500cm ⁻¹)
2	2920	2920	3355	O-H stretching vibration in carboxylic acid groups (2500-3500cm ⁻¹)
3	2851	2851	2920, 2853	O-H stretching vibration in carboxylic acid groups (2500-3500cm ⁻¹)
4	2123	2123	-	N=N=N group due to antisymmetric atretching (2160-2080cm ⁻¹)
5	1723	1721	-	C=O stretching in acid anhydrides (1765-1725cm ⁻¹) due to C=O stretching
6	1655	1655	1657, 1650	General presence of C=O groups stretching vibrations (1650-1800cm ⁻¹)
7	1639	1639	1639	C=O stretching in tertiary amides (1670-1630cm ⁻¹)
8	1603	1620	1609	Benzene ring stretching in aromatic compounds (1615-1590cm ⁻¹)
9	1562	-	-	NO ₂ in aliphatic nitro compounds due to antisymmetric stretching (1575-1545cm ⁻¹)
10	1439	-	-	OH in carboxylic acid groups due to in-plane OH bending (1440-1400cm ⁻¹)
11	1316	-	-	COO ⁻ due to symtric stretching (1400-1310cm ⁻¹)
12	1242	1162	1102	C-N stretching vibration in amines (1030-1330cm ⁻¹)
13	1035	1035	1037	C-N stretching vibration in amines (1030-1330cm ⁻¹)
14	724	-	-	Presence of -(CH ₂) _n - in hydrocarbons due to CH ₂ rocking in methylene chains (740-720cm ⁻¹)
15	678	-	-	O-C=O in carboxylic acid groups due to O-C=O bending (700-590cm ⁻¹); C-C-CHO in aldehydic compounds due to C-C-CHO bending (695-635cm ⁻¹)
16	659	-	-	O-C=O in carboxylic acid groups due to O-C=O bending (700-590cm ⁻¹); C-C-CHO in aldehydic compounds due to C-C-CHO bending (695-635cm ⁻¹)

REFERENCES

- [1] Ianišl, M., Tsekova, K. and Vasileva, S. (2006). Copper Biosorption by *Penicillium cyclospium*, Equilibrium and Modelling Study. *Biotechnology*, 195.
- [2] Arshad, M., Zafar, M. N., Younis, S., and Nadeem, R. (2008). The Use of Neem Biomass for the Biosorption of Zinc from Aqueous Solutions, *Journal of Hazardous Materials*, 157: 534–540. <http://dx.doi.org/10.1016/j.jhazmat.2008.01.017>
- [3] Gupta, V.K. and Suha S. (2009). Application of low-cost adsorbents for dye removal: a review. *Journal of Environmental Management*, 90, 2313-2342. <http://dx.doi.org/10.1016/j.jenvman.2008.11.017>
- [4] Monvisade, P. and Siriphannon, P. (2009). Chitosan intercalated montmorillonite: Preparation, characterization and cationic dye adsorption. *Applied Clay Science*, 42:427-431. <http://dx.doi.org/10.1016/j.clay.2008.04.013>
- [5] Šćiban, M., Klačnja, M. and Škrbić, B. (2008). Adsorption of copper ions from water by modified agricultural by-products. *Desalination*, 229:170-180. <http://dx.doi.org/10.1016/j.desal.2007.08.017>
- [6] Crini, G. (2006). Non-conventional low-cost adsorbents for dye removal: A review. *Bioresour. Technol.*, 97, 1061-1085. <http://dx.doi.org/10.1016/j.biortech.2005.05.001>
- [7] Ibrahim, M. B. and W. L. O. Jimoh (2008). Adsorption studies for the Removal of Cr(VI) ion from aqueous Solution. *Bayero Journal of Pure and Applied Sciences*. 1(1):99 – 103.
- [8] Ibrahim, M. B. and W. L. O. Jimoh (2012). Thermodynamics and Adsorption Isotherms for the Biosorption of Cr(VI), Ni(II) and Cd(II) onto Maize Cob. *ChemSearch Journal*, 3(1): 7 – 12.
- [9] Muhammad B. Ibrahim, Maje A. Haruna and Atika M. Ibrahim (2012). Optimization of Crystal Violet Dye Removal from Aqueous Solution using Agro Wastes. *ChemSearch Journal*, 3(1): 28 – 33.
- [10] Muhammad B. Ibrahim and Sadiq Sani (2014). Comparative Isotherms Studies on Adsorptive Removal of Congo Red from Wastewater by
- [11] Watermelon Rinds and Neem-tree Leaves, *Open Journal of Physical Chemistry*, 4(4):139 – 146.
- [12] Vimonses, V., Lei, S., Jin, B., Chow, C. W. K. and Saint, C. (2009). Kinetic study and equilibrium isotherm analysis of Congo red adsorption by clay materials. *Chemical Engineering Journal*, 148:354-364. <http://dx.doi.org/10.1016/j.cej.2008.09.009>
- [13] Wong, Y.C., Szeto, Y.S., Cheung, W.H. and McKay, G. (2004). Adsorption of acid dyes on chitosan—equilibrium isotherm analyses. *Process Biochemistry*, 39:695-704. [http://dx.doi.org/10.1016/S0032-9592\(03\)00152-3](http://dx.doi.org/10.1016/S0032-9592(03)00152-3)
- [14] Sharma, A. and Bhattacharyya, K. G. (2005) *Azadirachta indica* (Neem) leaf powder as a biosorbent for removal of Cd(II) from aqueous medium *Journal of Hazardous Materials B* 125 102–112. <http://dx.doi.org/10.1016/j.jhazmat.2005.05.012>
- [15] Sharma, N., Tiwari, D.P. and Singh, S. K. (2012). Decolourization of Synthetic Dyes by Agricultural Waste - A review. *International Journal of Scientific & Engineering Research*, 3 (2):1-10. <http://dx.doi.org/10.15373/22778179/MARCH2014/139>
- [16] Gopalakrishnan, K., Manivannan, V. and Jeyadoss, T. (2010). Comparative study of Zn(II), Cu(II) and Cr(VI) from textile dye effluent using sawdust and neem leaves powder. *E-Journal of Chemistry*, 7, S1, S504-S510. <http://dx.doi.org/10.1155/2010/506424>

- [17] Sluiter, A., Hames, B. Ruiz, R., Scarlata, C., Sluiter, J. and Templeton, D. (2005). *Determination of Ash in Biomass: Laboratory Analytical Procedure (LAP), Technical Report: NREL/TP-510-42622*, January 2008). National Renewable Energy Laboratory, United States of America.
- [18] Suyamboo, B.K. and Perumal R.S. (2012). Equilibrium, thermodynamic and kinetic studies on adsorption of a basic dye by *Citrullus Lanatus* rind. *Iranica Journal of Energy & Environment*, 3 (1), 23-34.
<http://dx.doi.org/10.5829/idosi.ijee.2012.03.01.0130>
- [19] Lian, L., Guo, L. and Guo, C. (2009). Adsorption of Congo red from aqueous solution on Cabentonite. *Journal of Hazardous Materials*, 161, 126-131.
<http://dx.doi.org/10.1016/j.jhazmat.2008.03.063>
- [20] Patil, S., Renukdas, S. and Patel, N. (2011). Removal of methylene blue from aqueous solutions by adsorption using teak tree (*Tectona grandis*) bark powder. *International Journal of Environmental Sciences*, 1:711-725.
- [21] Abdullah, N.M., Othaman, R., Abdullah, I., Jon, N. and Baharum, A. (2012). Studies on the adsorption of phenol red dye using silica-filled enr/pvc beads. *Journal of Emerging Trends in Engineering and Applied Sciences (JETEAS)*, 3, 5, 845-850.